Paull, C.K., Matsumoto, R., Wallace, P.J., and Dillon, W.P. (Eds.), 2000
Proceedings of the Ocean Drilling Program, Scientific Results, Vol. 164

38. ROCK MAGNETISM OF THE DIAPIR SITES (SITES 991, 992, 993, AND 996), CAROLINA RISE AND BLAKE RIDGE[1]

Robert J. Musgrave[2] and Yoshihisa Hiroki[3]

ABSTRACT

Magnetic diagenesis, involving a sequence of iron reduction steps resulting in initial authigenesis of magnetite and progressing through reduction to greigite and on to pyrite, can be traced in Leg 164 sites by downhole changes in susceptibility, the hysteresis parameter D_{JH}, and coercivity spectra. An undisturbed reference site on the Blake Ridge (Site 995) shows an initial increase in susceptibility between 0 and 4 mbsf, consistent with authigenesis of fine-grained magnetite and greigite, followed by almost complete reduction to pyrite below 4 mbsf. Site 991 shows a similar pattern restricted to Unit I; Unit II, although it commences at only 2 mbsf, is thoroughly reduced, reflecting the removal of material in a slide prior to the deposition of Unit I. At Site 992 the authigenesis of magnetite in Unit I has a different character; it is dominated by single-domain magnetite, suggesting that the multiple remobilization and redeposition of Unit I sediments at this site may have encouraged the growth of slightly larger magnetite grains, perhaps by incorporation of additional sulfate in the redeposited sediments. Unit I sediments at Site 992 have never been exhaustively reduced, suggesting that they were not buried by more than about 4 m prior to remobilization. In contrast, the entire sequence at both Sites 993 and 996 are thoroughly reduced. At Site 993 this reflects the exhumation of the site, which was previously estimated by physical properties (shear strength) measurements to be 50–80 m. Site 996 has not been exhumed significantly; instead reduction here has proceeded extensively even near the seafloor because of the supply of methane along a fault.

INTRODUCTION

Leg 164 was the first Ocean Drilling Program (ODP) leg to have the study of the occurrence of natural gas hydrates in sediments as its principal objective. A series of sites were drilled on the Blake Ridge, a Neogene and Quaternary sediment drift (Tucholke et al., 1977) comprising hemipelagic silt and contourites, and on a sector of the southern Carolina Rise penetrated by one of a series of diapirs that form a linear array extending for more than 200 km along the base of the rise. Gas hydrate had been previously recovered in Deep Sea Drilling Project (DSDP) drilling on the Blake Ridge (Gradstein and Sheridan, 1983). A bottom-simulating reflector (BSR), interpreted as indicating the base of an interval of gas hydrate accumulation, is prominently developed on the Blake Ridge and Carolina Rise (Shipley et al., 1979; Dillon and Paull, 1983).

Extending from the Carolina Rise to the Hatteras Abyssal Plain is the Cape Fear Slide, one of the largest continental margin slide features in the world (Popenoe et al., 1993). Near its headwall scarp, the sole of the Cape Fear Slide is breached by the Cape Fear Diapir. Leg 164 drilled three sites (Sites 991, 992, and 993) near the Cape Fear Diapir (Shipboard Scientific Party, 1996c) to investigate the relationship (if any) between the formation of the slide and the intrusion of the diapir, and to test the hypothesis that decomposition of the base of a hydrate layer might have fluidized sediments to mobilize the base of the slide (Carpenter, 1981; Cashman and Popenoe, 1985; Popenoe et al., 1993; Schmuck and Paul, 1993).

At the top of the Blake Ridge, where it merges with the Carolina Rise, the Blake Ridge diapir produces a topographic bulge in the overlying sediments, and is marked by a pockmarked seafloor with actively venting faults and associated chemosynthetic communities (Paull et al., 1995). Objectives at Site 996 were to investigate methane migration and gas hydrate formation in a fault zone where the methane may be sourced from decomposition of hydrate below. Site 996 also provided abundant samples of hydrate recovered in cores (Shipboard Scientific Party, 1996e).

Rock-magnetic investigations on samples from Leg 164 have focused on the bacterial mediation of the diagenesis of magnetic oxides and sulfides. At the Blake Ridge sites (Sites 994, 995, and 997), these studies have confirmed the rock-magnetic signature of enhanced bacterial activity at the BSR and have indicated a close correspondence between rock magnetic parameters that reflect oxidation state and grain size in the magnetic mineralogy (magnetite and greigite) and the patterns of biological activity in bacterial cultures isolated from these samples (Musgrave, Goodman, Parkes, et al., 1997).

The diapir sites, Sites 991, 992, 993, and 996, provide a different setting from the Blake Ridge sites. No BSR is present at the Cape Fear Diapir sites, and drilling at Site 996 was restricted to shallower than 63 m below seafloor (mbsf). Hence none of the diapir sites involves penetration of a BSR. In contrast to the Blake Ridge sites, however, all four diapir sites involve substantial disturbance to the sequence of sediment accumulation and early magnetic diagenesis typical of reduced marine sediments. At Sites 991, 992, and 993, this disturbance is physical, and results from diapir emplacement, from deformation related to repeated slumping, and from exhumation following the slumping of the Cape Fear Slide (Shipboard Scientific Party, 1996b). At Site 996, methane is being vented to the seafloor along a fault that taps a BSR that is domed upwards around the Blake Ridge Diapir. The fault-enhanced transport of methane into the zone of seawater diffusion appears to result in very active sulfate reduction, including the production of large quantities of H_2S, similar to the situation observed at Site 892 on Leg 146 (Shipboard Scientific Party, 1994; Housen and Musgrave, 1996).

For each of these diapir sites, rock-magnetic studies were directed toward contrasting the disturbed rock-magnetic depth profile with the undisturbed profile observed at the Blake Ridge sites.

[1]Paull, C.K., Matsumoto, R., Wallace, P.J., and Dillon, W.P. (Eds.), 2000. *Proc. ODP, Sci. Results,* 164: College Station, TX (Ocean Drilling Program).
[2]Department of Earth Sciences, La Trobe University, Bundoora, VIC 3083, Australia. R.Musgrave@latrobe.edu.au
[3]Department of Earth Science, Osaka Kyoiku University, 4-698-1, Asahigaoka, Kashiwara, Osaka 582, Japan.

METHODS

Shipboard rock-magnetic methods included a series of anhysteretic remanence (ARM) acquisition and demagnetization measurements on discrete plastic box samples (Shipboard Scientific Party, 1996a). Remanences were measured on a Molspin spinner magnetometer. ARM was imparted using a DTECH bias coil mounted in a Schonstedt GSD-1 alternating-field (AF) demagnetizer, with an effective AF operating limit of 90 mT. Discrete samples, which had already been AF demagnetized, were exposed to a bias field of 0.1 mT in AF-acquisition windows 10 mT wide, centered on steps of 5 mT up to 85 mT to impart partial ARMs (pARM). A final bulk ARM was imparted over a complete 90-mT demagnetization cycle, after which some samples were again demagnetized in 10-mT steps up to 90 mT (demagnetization of ARM, dARM). Shipboard time constraints limited dARM measurements to Sites 991, 992, and 994.

Magnetic susceptibility was measured on unsplit APC cores by a Bartington MS2 susceptibility meter with a MS1/CX80 whole-core sensor attached to the multisensor track (MST), and on discrete samples with a Bartington MS2 system using a MS1B well sensor set to its "0.1 SI" scale.

Shipboard rock-magnetic samples were processed as soon as possible after sampling (within a few days at most), to minimize alteration to the magnetic mineralogy through oxidation. Samples destined for shore-based rock-magnetic analysis were collected and prepared according to one of three regimes.

1. A set of samples from Site 995 that were dedicated for shore-based microbiological and rock-magnetic analysis was taken immediately following sectioning of the core on the catwalk and was stored in an anoxic atmosphere, using Anaerocult packaging. After opening of the packaging, a split of each sample was freeze dried and stored in a sterile plastic pot with an oxygen-free nitrogen headspace. Rock-magnetic specimens were prepared from these splits immediately after opening of the plastic pots, and hysteresis analysis was completed within an hour of exposure of the samples to the air. This set of samples, which should show minimal effects of post-coring oxidation on the magnetic mineralogy, is referred to below as the "A995 set."
2. A second set of samples from Site 995 (originally sampled for magnetostratigraphy) were also subjected to rock-magnetic analysis; however, these samples were not protected from exposure to the air during storage or specimen preparation. These samples are referred to as the "B995 set." Oxidation in samples stored in this way has been noted to result in changes in rock-magnetic parameters. In particular, the ferrimagnetic sulfide greigite has been reported to decompose rapidly in air in some samples, resulting in a decrease in saturation magnetization and a change in coercivity (Snowball and Thompson, 1990; Kalcheva et al., 1990).
3. Samples for shore-based rock-magnetic analysis from Sites 991, 992, 993, and 996 were all stored in Anaerocult packaging. After opening of the packaging, samples were stored at <4°C, and rock-magnetic specimens were prepared and processed as soon as possible after opening of the package (maximum delays were a few days). These samples should also show relatively little influence of post-coring oxidation.

Hysteresis parameters were determined in the La Trobe University PALM laboratory using a Molspin NUVO vibrating sample magnetometer (VSM). Saturation magnetization (J_s), saturation remanence (J_{rs}), and coercivity (H_c) were determined from hysteresis loops to >800 mT (sufficient to achieve saturation in all samples), after subtraction of the paramagnetic contribution determined from the M/H gradient at >500 mT. Coercivity of remanence (H_{cr}) was also determined on the VSM, by imparting an IRM at 800 mT, and then applying successively increasing field steps in the opposite directions; remanence was determined by turning the applied field off after each step. Because many of the samples were very weakly magnetized, with J_{rs} frequently less than 50 $\mu A\,m^2\,kg^{-1}$, the signal-to-noise ratio of coercivity of remanence was improved by averaging repeated measurements.

Stages in the reduction sequence of the magnetic mineralogy were traced downhole at each of the sites through changes in coercivity and saturation magnetization indices, which indicate changes in domain state (and hence magnetic grain size) and mineralogy. Histograms of pARM and dARM directly indicate changes in the distribution of coercivity of remanence, and can reflect the presence of distinct populations of magnetic phases. Hysteresis parameters can be combined in a Day plot (Day et al., 1977), defining fields corresponding to ferrimagnet domain states. The index $D_{JH} = (J_{rs}/J_s)/(H_{cr}/H_c)$ (Housen and Musgrave, 1996) indicates position on the Day plot, and so allows domain state to be plotted as a function of depth. A single domain (SD) dominated assembly is indicated by values of $D_{JH} > 0.33$; $D_{JH} < 0.0125$ indicates multidomain (MD) or superparamagnetic (SPM) populations, and intermediate values of D_{JH} indicate a net pseudosingle domain (PSD) state, or a mix of SD and SPM or MD populations. Domain state reflects grain size: in magnetite, SD grains range between about 50 nm and 1 μm; PSD typically ranges between 0.1 and 10 μm; MD > 10 μm; and SPM < 50 nm.

REDUCTION SEQUENCE AT SITE 995—AN UNDISTURBED REFERENCE SECTION

Sedimentation at the Blake Ridge sites (Sites 994, 995, and 997) was uninterrupted through the late Pliocene and Quaternary, resulting in an undeformed and continuous sequence of nannofossil-rich clays extending below 100 mbsf at all three sites. Interstitial methane and sulfate profiles indicate limited seawater diffusion and no evidence of significant methane transport into the sulfate reduction zone, in contrast with Site 996. As a consequence, the Blake Ridge sites show the normal pattern of magnetic diagenesis in reduced marine sediments, which is illustrated by the MST susceptibility record for the upper part of Site 995 (Fig. 1). Magnetic diagenesis in reduced sediments involves a series of iron reduction steps within the first few meters below the seafloor, beginning with authigenesis of magnetite, through generation of incompletely reduced iron sulfides, including the ferrimagnetic phase greigite, to complete iron reduction to pyrite (Canfield and Berner, 1987; Karlin, 1990; Leslie et al., 1990). Susceptibility in the three Blake Ridge sites increases from the seafloor to about 2 mbsf. The increase in susceptibility presumably results from authigenesis of magnetite, adding to the depositional load of detrital magnetite. A decrease in susceptibility immediately below this peak reflects a first stage of further reduction of magnetite to sulfides; a second peak at about 3 mbsf may represent growth of greigite, before susceptibility precipitously declines at about 3.75 mbsf as iron sulfides are fully reduced to pyrite, which is paramagnetic.

On a Day plot, samples from the A995 set from Site 995 plot in the PSD field, or just to the right of the PSD field, indicating an admixture of MD or SPM grains with PSD grains (Fig. 2A). Samples migrate across the field in a systematic way with increasing depth, following a path that suggests an increase in the proportion of SPM grains from 0.13 to 0.6 mbsf, a decrease in the proportion of SPM grains from 0.6 to 3.83 mbsf, and an increase in the proportion of MD grains from 3.83 to 28.60 mbsf. Figure 3 shows the downhole behavior of D_{JH} for the A995 set, which summarizes the trends seen in the Day plot.

Because the A995 set of anoxically stored samples is small, we chose to examine the rock magnetism of the larger B995 set, to see whether this pattern of behavior could be confirmed. However, the

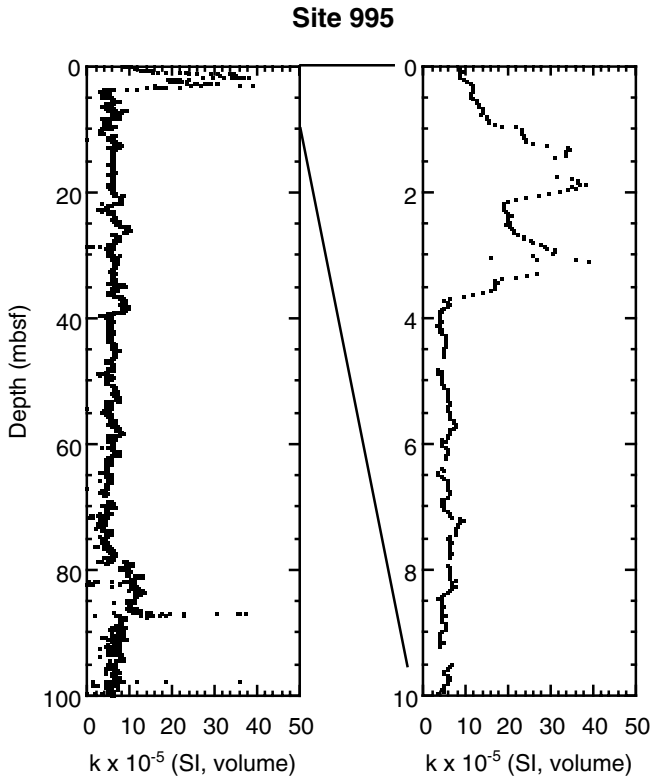

Figure 1. MST susceptibility record in the upper part of the sequence at Site 995.

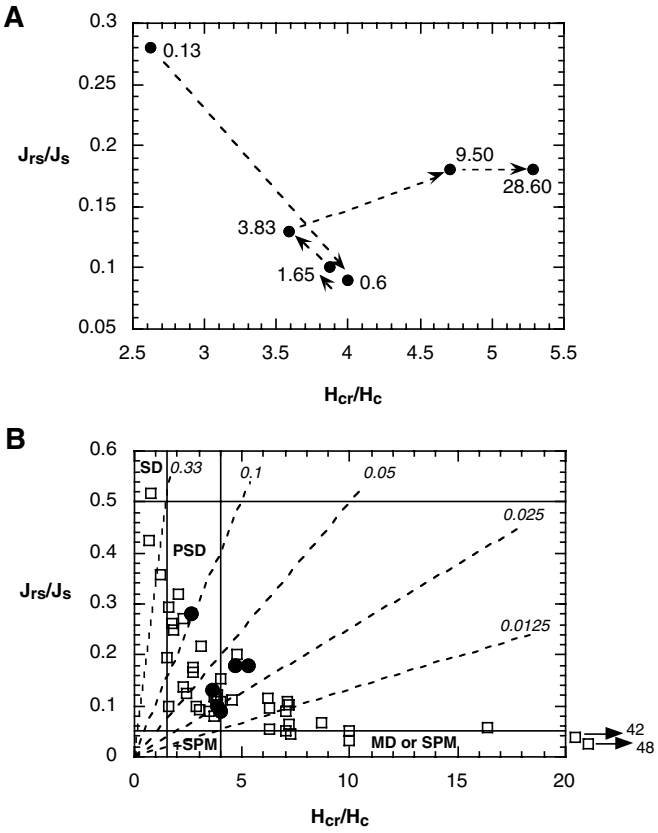

Figure 2. Day plots of hysteresis parameters of samples from Site 995. **A.** Samples from set A995, stored in anoxic conditions to prevent oxidation. Depths in meters below seafloor for each sample are indicated; arrows indicate the sequence with increasing sub-bottom depth. **B.** Samples from both sets A995 (solid symbols) and B995 (open symbols); B995 samples were not protected from oxidation. Note the change in both vertical and horizontal scales from Part A. Domain state fields are indicated on the plot: SD = single domain, PSD = pseudosingle domain, MD or SPM = common field for multidomain and superparamagnetic assemblages, +SPM = field representing addition of large proportions of SPM grains to an otherwise PSD or SD assemblage. Dashed lines join equal values of D_{JH}, indicated in italics.

B995 set plots over a much wider region on a Day plot than does the A995 set (Fig. 2B), and the B995 samples do not show a systematic trend. The origin of the differing behavior of the two sets is suggested by comparison of the downhole distribution of the rock-magnetic parameters J_{rs}, J_s, H_{cr}, and H_c of the two sample sets (Fig. 3). Below the susceptibility-decrease horizon at 3.75 mbsf, most B995 samples have J_{rs} (and less distinctly J_s) values that are lower than the A995 samples. The difference between the two sets can be explained if greigite makes up a significant proponent of the remanence-carrying (i.e., larger than SPM) grains below 3.75 mbsf. Oxidation of greigite in the B995 samples would have produced a decrease in saturation remanence and magnetization. Oxidation also appears to have reduced and scattered coercivity of remanence, and scattered coercivity to both higher and lower values; such apparent changes to H_{cr} and H_c may merely reflect the very low saturation remanences of many of the B995 samples, which makes accurate determination of coercivity parameters very difficult. Scatter in both H_c and H_{cr} results in scattered, nonsystematic behavior in D_{JH} for the B995 samples.

Despite its small size, the A995 set appears to be a more faithful record of the in situ magnetic diagenesis in the reference site than the B995 set. Surprisingly, the increase in susceptibility over the first 2 mbsf at Site 995 is accompanied by an initial decrease in H_c, H_{cr}, and D_{JH}, indicating a decrease in the proportion of more stable, single-domain–sized ferrimagnet grains in the total magnetic population (Fig. 3). At the seafloor, D_{JH} has a value >0.1, representing a position in the middle of the PSD field. At about 0.6 mbsf, D_{JH} reaches a minimum of about 0.02, which represents an average ferrimagnet domain state just within the PSD field, very close to the boundary with the SPM/MD fields. This occurs despite an increase in saturation magnetization, and so may represent addition of SPM or near-SPM grains, occurring at the same time as SD magnetite is being lost. Magnetotactic bacteria have been reported to produce magnetite and greigite grains in the SD size range (e.g., Heywood et al., 1990), whereas individual ferrimagnet grains produced by dissimilatory bacteria are commonly smaller, in or near the superparamagnetic range (Lovley et al., 1987; Lovley and Phillips, 1988). Reduction in anaerobic sediments from the Chile margin at ODP Site 863 (Musgrave et al., 1995) also appears to have involved production of near-SPM greigite grains.

In the set of anaerobically stored samples, coercivity and D_{JH} recover slightly over the interval from 1 to 4 mbsf. Both saturation magnetization and saturation remanence initially increase to 2 mbsf, and then decrease sharply. The change in D_{JH} represents a small shift away from the SPM/MD field, and the trends in both D_{JH} and saturation magnetizations below 2 mbsf could be explained by further reduction of ultra-fine-grained (near-superparamagnetic) magnetite and/or greigite to pyrite.

The subsidiary peak in susceptibility at 3–4 mbsf may represent an intermediate step in which greigite is generated, before further reduction to pyrite. At least some of this greigite may be SD in size as indicated by the trend in D_{JH} over this interval and by the evidence that remanence-carrying greigite has been destroyed by oxidation below this depth. Below 4 mbsf, and extending down to the bottom of Site 995 at 700 mbsf, D_{JH} mostly remains below 0.05, near the boundary between the PSD and SPM/MD fields. The trend on the Day plot

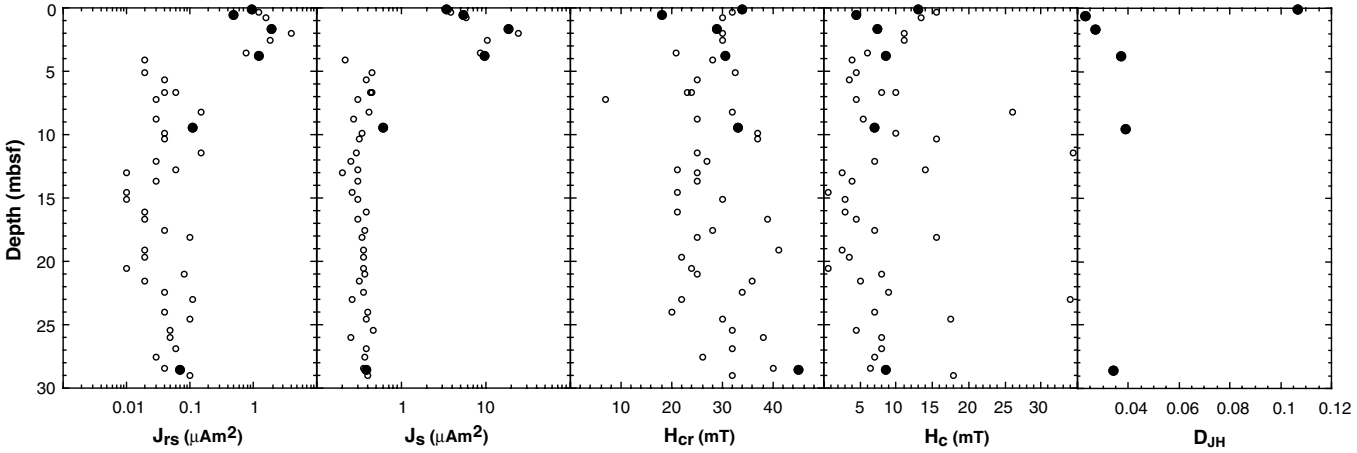

Figure 3. Hysteresis parameters in upper part of the sequence at Site 995. J_{rs} = saturation remanence, J_s = saturation magnetization, H_{cr} = coercivity of remanence, H_c = coercivity, and D_{JH}. Results from samples from sets A995 (solid symbols) and B995 (open symbols) are compared for J_{rs}, J_s, H_{cr}, and H_c. D_{JH} shows only results from set A995; D_{JH} from set B995 is highly scattered. Coercivity is in mT. J_{rs} and J_s are given as moments in μAm^2 for samples of ~1 g.

suggests further conversion of SD or PSD greigite and/or magnetite grains to pyrite, leaving a residuum of larger, MD grains. Saturation remanence, saturation magnetization, pARM intensity, and susceptibility all decrease sharply below 4 mbsf, to substantially lower than the near-seafloor values (although scattered exceptional samples show higher values deeper in the sequence). Little of the original detrital load of magnetite survives below 4 mbsf, and the finer fraction of any ferrimagnetic minerals present—both any PSD or SD grains that may have been present in the detrital magnetite, and SPM or SD magnetite and greigite produced in the earlier stages of reduction—has been mostly reduced through to pyrite.

Samples from less than 1 mbsf have a single coercivity population, shown by histograms of pARM and dARM (Fig. 4). The peak in these histograms occurs at about 25–35 mT, typical of MD to PSD magnetite, consistent with a detrital origin. Below 4 mbsf pARM and dARM histograms fall into two classes: they are either strongly left-skewed, with a single peak at about 15 mT, or they are bimodal, with peaks at 15 and 35–55 mT. The left-skewed samples may be explained by preferential loss of finer grained, SD and PSD magnetite, relative to the coarser MD fraction. The samples with two peaks suggest two populations of magnetic phases. Thermal demagnetization of multicomponent isothermal remanence (Shipboard Scientific Party, 1996d) indicates the presence in these samples of a thermally metastable phase (decomposing at 250°–300°C) with coercivity higher than magnetite, tentatively identified as greigite. The presence of greigite was positively confirmed by XRD in Site 995 samples. It is likely that the higher coercivity population present in these samples includes SD greigite.

SITES 991 AND 992

At Site 991, the uppermost part of the sequence (lithostratigraphic Unit I, 0–2.05 mbsf) is an undisturbed late Pleistocene to ?Holocene nannofossil-rich clay that overlies a disturbed early Pliocene to late Pleistocene interval containing layers of clay conglomerates (Unit II, 2.05 mbsf to bottom of hole, 47.66 mbsf). At Site 992, a similar disturbed interval containing clay conglomerates extends from the seafloor to 9.10 mbsf and has a Pleistocene to ?Holocene age; in concordance with ODP convention, this becomes Unit I for Site 992, even though it more closely resembles Unit II of Site 991. Unit II at Site 992 is an interval of undisturbed, diatom- and nannofossil-rich clay, restricted to the middle late Miocene, and extending to the base of the hole at 50.75 mbsf.

Slumping and mass transport are indicated by the disturbed intervals represented by Unit II at Site 991 and Unit I at Site 992. These represent repeated slumping and transport events (at least three within the Miocene to Pleistocene at Site 991). Much of the section between the upper Miocene and the Pleistocene at Site 992 (which lies above the summit of the diapir) may have been removed downslope by repeated slumping. Site 991, which is located on the flank of the diapir, may have accumulated multiple mass-transport deposits from sediment failures further upslope on the diapir's crest. Alternatively, all of the mass-transport deposits at Sites 991 and 992 may have been emplaced as part of a larger Cape Fear Slide complex (Shipboard Scientific Party, 1996c).

At Site 991, the interval of increased susceptibility is restricted to the uppermost, undisturbed lithostratigraphic unit (Fig. 5). The susceptibility shows a single peak instead of the double or multiple peaks seen at Site 995. The D_{JH} profile, however, is broadly similar to Site 995 (Fig. 6); D_{JH} is a maximum in the shallowest sample (0.4 mbsf) with a value of 0.085, slightly lower than the maximum at Site 995 but still near the middle of the PSD field. D_{JH} declines sharply below Unit I to a minimum of 0.006 at 3.6 mbsf, rises slightly between 6.5 and 13 mbsf to about 0.035, then settles down to less than 0.02 for the remainder of the hole. Coercivity spectra for pARM and dARM indicate an initial population with a peak at around 25–40 mT at 0.4 mbsf, which becomes sharply left skewed at 3.4 mbsf, and exhibits a bimodal coercivity distribution for some samples deeper in the hole (Fig. 7).

Susceptibility at Site 992 forms a broader initial high (Fig. 5), with a series of peaks between 0 and 6 mbsf. Paradoxically, D_{JH} is a minimum near the seafloor (0.03 at 1.2 mbsf) and increases sharply within the interval of high susceptibility to values around 0.5 (Fig. 6), well within the SD field. Coercivity spectra in this interval mirror D_{JH}, with strongly right-skewed pARM and dARM histograms indicating peak coercivities at about 65–70 mT (Figs. 8A, 8B). Below the susceptibility maximum D_{JH} declines sharply to less than 0.03 (in the PSD field, near the boundary of the SPM/MD field), with the exception of a sample at 15.9 mbsf, where D_{JH} lies near the middle of the PSD field, at about 0.08. Coercivity spectra in samples below the high-susceptibility interval all show weakly developed bimodal behavior (Figs. 8C, 8D).

SITE 993

The cored sedimentary section at Site 993 is largely homogeneous nannofossil-rich clay, and so only a single lithostratigraphic unit

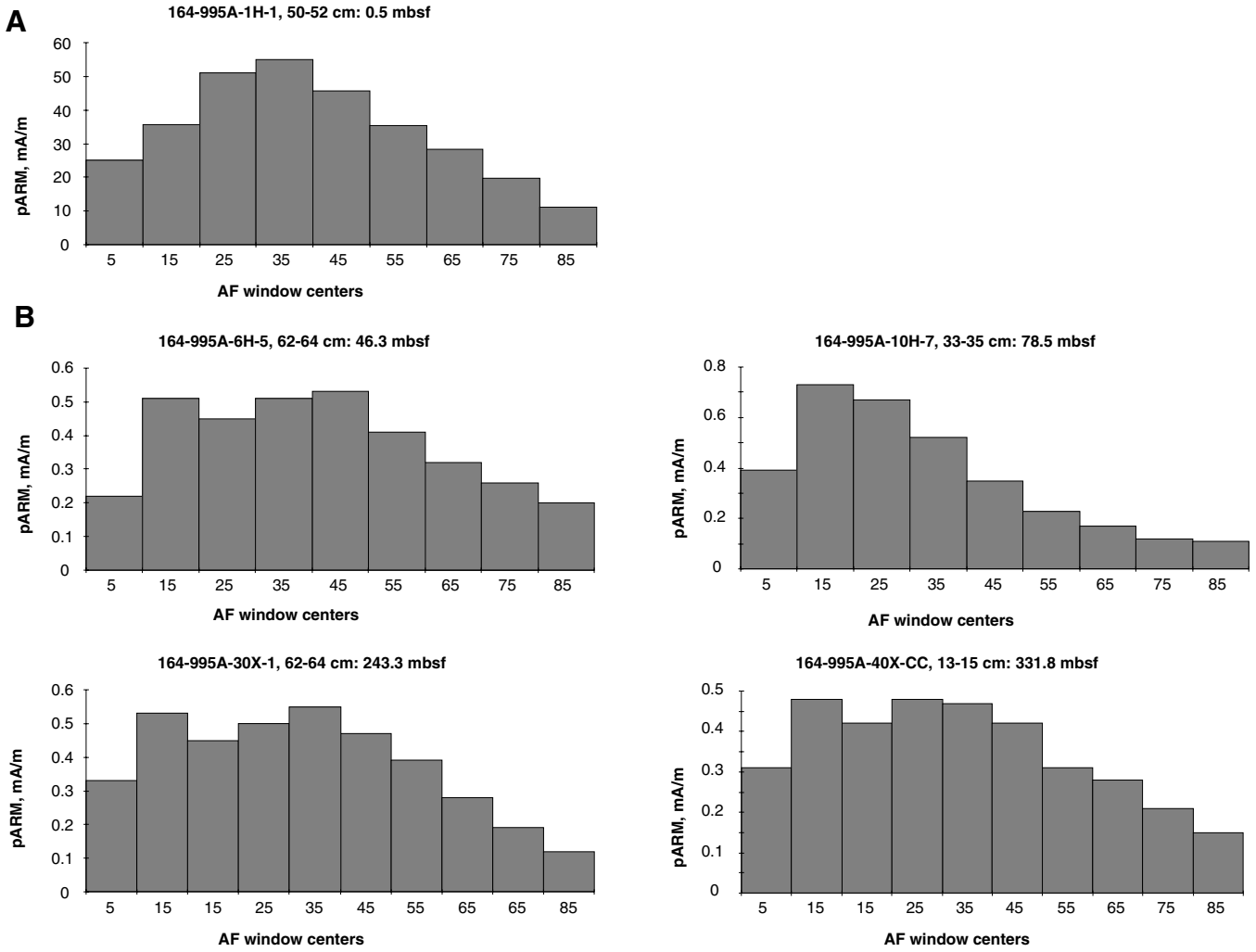

Figure 4. Histograms showing coercivity spectra at Site 995 as acquisition of pARM. **A.** Sample above the high-susceptibility interval. **B.** Samples below the high-susceptibility interval.

(Unit I, 0–42.7 mbsf) was defined for this site. The uppermost 6 cm below seafloor yielded a latest Quaternary nannofossil flora; the remainder of the sequence has an early late Miocene (Zone CN7 to Subzone CN8a) assemblage (Shipboard Scientific Party, 1996c), indicating a substantial time break consistent with removal of part of the sequence by mass-wasting processes, either locally on the flanks of the Blake Ridge diapir or as part of the movement of the Cape Fear Slide.

Susceptibility at Site 993 shows no near-surface high (Fig. 5). Peaks scattered through the MST record probably only represent rust contamination around biscuits in the XCB cores (Shipboard Scientific Party, 1996c). Throughout the section, D_{JH} is mostly below 0.03, with an isolated value of 0.055 at 11 mbsf (Fig. 6). In other words, the whole of the section at Site 993 has a rock-magnetic character like that of Unit II at Sites 991 and 992.

SITE 996

Five holes were drilled at Site 996: Holes 996A, 996B, and 996C were drilled beneath an active chemosynthetic community, and Holes 996D and 996E were drilled about 40 m away, on the flanks of the community. A single lithostratigraphic unit was recognized, based on the combined observations from all five holes. This unit extends from the seafloor to 63.0 mbsf and is aged from early Pleistocene to Holocene and comprises nannofossil-bearing silty clay and nannofossil-rich clay, with up to 2-m-thick beds of partially cemented shell fragments associated with the biological community at Holes 996A, 996B, and 996C (Shipboard Scientific Party, 1996e).

Susceptibility at Site 996 shows no near-surface peak (Fig. 5), and D_{JH} remains uniformly low (Fig. 6), never exceeding 0.02 except near the base of Hole 996A, where D_{JH} reaches 0.03 at 59.6 mbsf. Coercivity spectra from throughout Site 996 are usually left skewed, but include a substantial fraction extending to high coercivities (Fig. 9). This may reflect the presence of SD greigite, or alternatively may indicate survival of some detrital hematite. Resistance of hematite to reductive diagenesis in greigite-bearing sediments has been reported by Reynolds et al. (1994).

DISCUSSION

At Site 991, the break between the undisturbed Unit I and the strongly disturbed Unit II, which includes soft-sediment deformation features and clay conglomerates, is taken to represent the sole of the last slide to affect this site. Sediments below this slide have overconsolidated physical properties; in rock magnetism, the time-break between the deposition of Units I and II appears as a small discontinuity

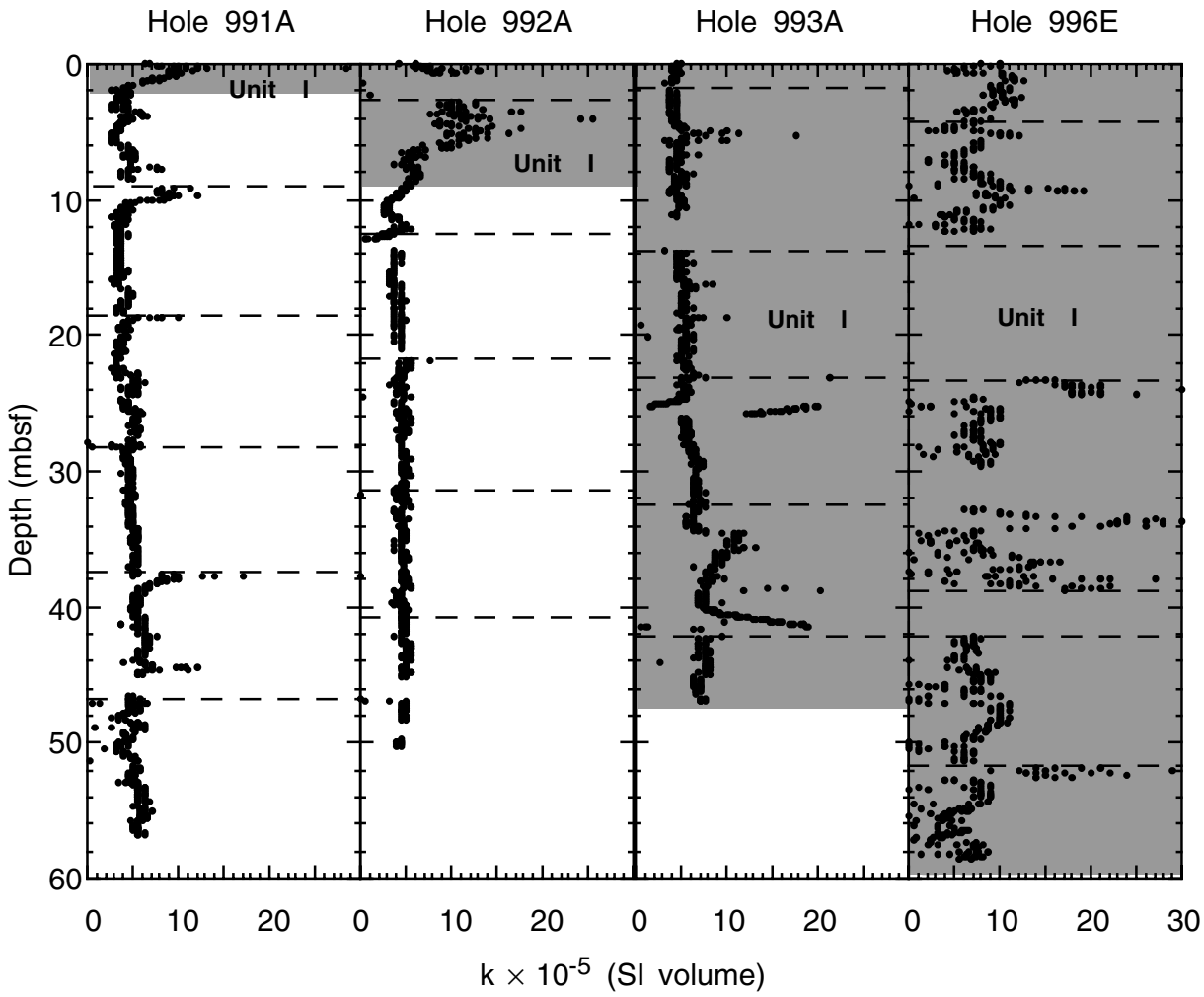

Figure 5. MST susceptibility at Sites 991, 992, 993, and 996.

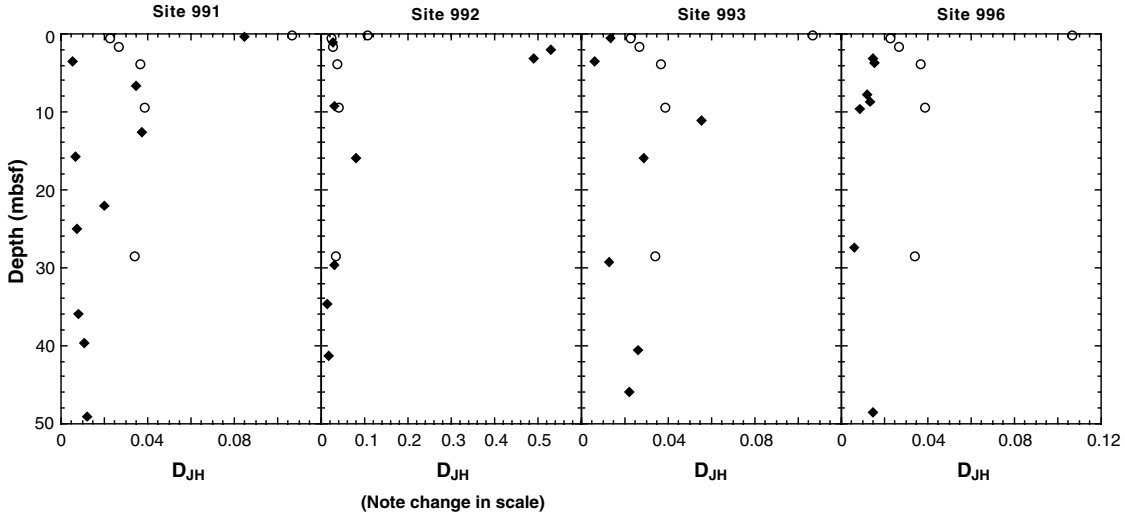

Figure 6. D_{JH} plotted against sub-bottom depth at Site 991, Site 992, Site 993, and Site 996. Results from each of the diapir sites (solid symbols) are compared with results from Site 995 (open symbols). Note the change in D_{JH} scale for Site 992, resulting from very high D_{JH} values in Unit I at this site.

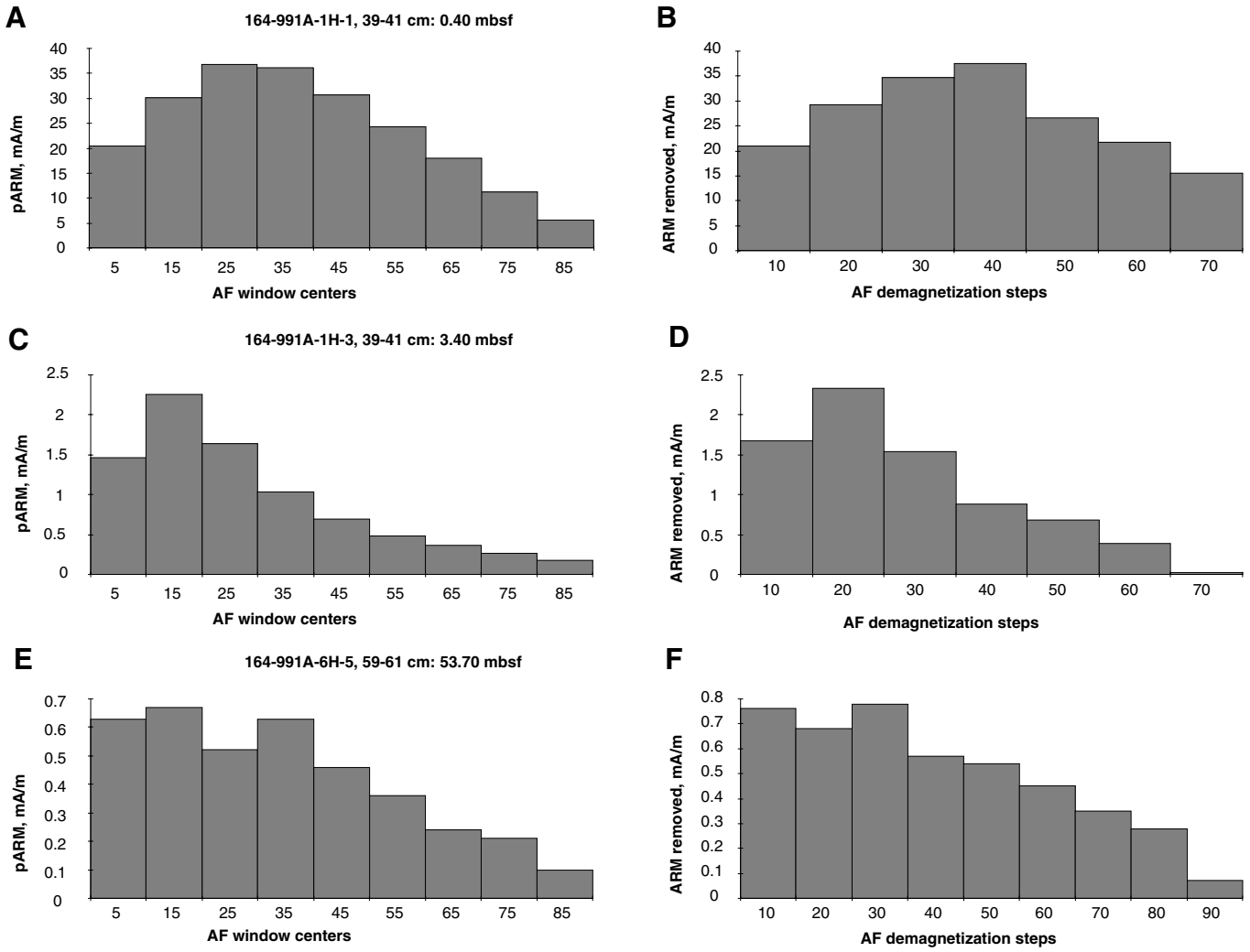

Figure 7. Coercivity spectra at Site 991, shown as pARM acquisition and ARM demagnetization (dARM) histograms. (**A**) pARM and (**B**) dARM of Sample 164-991A-1H-1, 39–41 cm (0.40 mbsf); (**C**) pARM and (**D**) dARM of Sample 164-991A-1H-3, 39–41 cm (3.40 mbsf); (**E**) pARM and (**F**) dARM of Sample 164-991A-6H-5, 59–61 cm (53.70 mbsf).

in the reduction pattern expressed by the susceptibility record, so that Unit II sediments have completed the magnetite-greigite-pyrite reduction sequence at a depth 2 m shallower than at the reference Site 995.

Disturbance is different at Site 992; here, Unit I is itself composed of clay conglomerates, involving soft-sediment deformation, displacement and redeposition. Rock magnetism suggests that authigenesis in Unit I at Site 992 results in an SD-dominated ferrimagnet population (D_{JH} around 0.5). This contrasts with Unit I at Site 991 and the interval above 2 mbsf at Site 995, where D_{JH} values do not indicate authigenic addition of SD-sized ferrimagnets. The magnetic diagenesis in Unit I at Site 992 may represent a more extreme form of the situation that appears to apply at around 3 mbsf at Site 995, where the second peak in susceptibility seems to involve generation of some SD- or near-SD–sized greigite. It is not clear why growth of large proportions of SD-sized grains should characterize Unit I at Site 992. It may be that the multiple displacements and assemblies of the sequence in Unit I at Site 992 have refreshed the supply of sulfate through to about 6 mbsf, making more sulfate available than was supplied at other sites from initial deposition and later diffusion. This may have encouraged a different style of bacterial activity (perhaps involving a different balance of species or metabolic pathways), resulting in greater proportions of larger magnetite and/or greigite grains, in the SD-size range. What is clear is that the redeposited sediments in Unit I at Site 992 had not already been fully reduced prior to redeposition; hence, these sediments have not been buried more than 4 mbsf prior to remobilization. This appears to conflict with physical properties evidence (Shipboard Scientific Party, 1996c), suggesting about 4 m of overburden have been removed at Site 992. It may be that the increased strength of the Site 992 sequence results from transport and redeposition mechanisms, rather than significant prior burial.

In contrast, the entire sequence at Site 993 has been completely reduced prior to its later exhumation, consistent with physical properties evidence for the stripping of 50–80 m of overburden.

Near-surface reduction is also unusually complete at Site 996, but this does not reflect removal of an overburden. Instead, the supply of methane via the fault at this site, greatly exceeding local microbial methane production or supply by normal diffusion, has pushed the magnetite-greigite-pyrite reduction series close to complete reduction to pyrite even at very shallow depths below the seafloor.

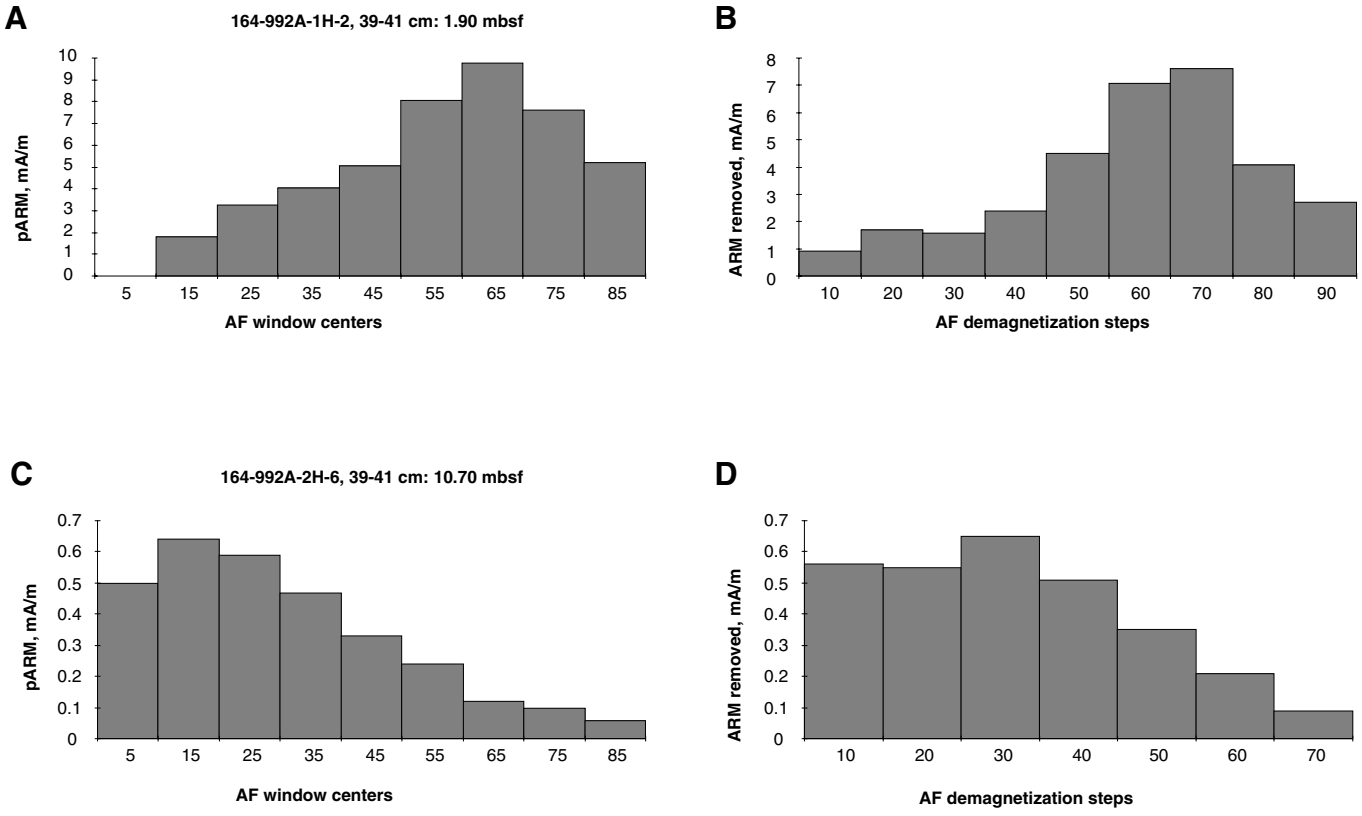

Figure 8. Coercivity spectra at Site 992. (**A**) pARM and (**B**) dARM of Sample 164-992A-1H-2, 39–41 cm (1.90 mbsf); (**C**) pARM and (**D**) dARM of Sample 164-992A-2H-6, 39–41 cm (10.70 mbsf).

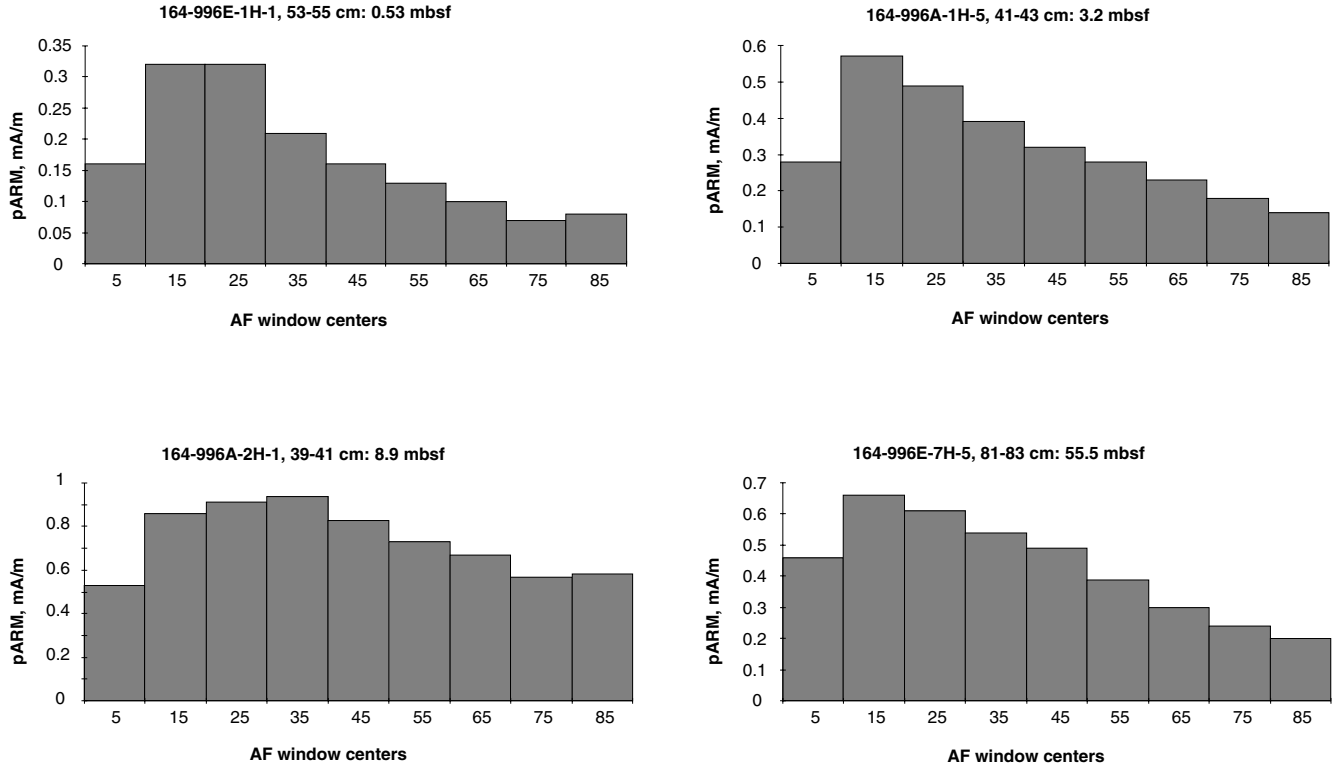

Figure 9. Coercivity spectra at Site 996, illustrated by pARM acquisition of Samples 164-996E-1H-1, 53–55 cm (0.53 mbsf), 164-996A-1H-5, 41–43 cm (3.2 mbsf), 164-996A-2H-1, 39–41 cm (8.90 mbsf), and 164-996E-7H-5, 81–83 cm (55.50 mbsf).

ACKNOWLEDGMENTS

We would like to express our thanks to the tireless and resourceful technical staff of the *JOIDES Resolution*, and particularly to our Leg 164 paleomagnetic technician, Margaret Hastedt. Margaret's mastery of the instrumentation in the laboratory, unfailing good humor, and supply of Madman comics made her a pleasure to work with. Shore-based analysis was conducted at the La Trobe University Palaeo/Archaeo/Litho-Magnetic laboratory (the "PALM" lab), as part of a project funded by the Australian Research Council. Y.H. thanks the Australian Academy of Science for its support as part of an exchange program with the Japan Society for the Promotion of Science. We would also like to thank the two reviewers, Bill Owen and Joe Stoner, for their constructive comments.

REFERENCES

Canfield, D.E., and Berner, R.A., 1987. Dissolution and pyritization of magnetite in anoxic marine sediments. *Geochim. Cosmochim. Acta,* 51:645–659.

Carpenter, G.B., 1981. Coincident sediment slump/clathrate complexes on the U.S. Atlantic continental slope. *Geo-Mar. Lett.,* 1:29–32.

Cashman, K.V., and Popenoe, P., 1985. Slumping and shallow faulting related to the presence of salt on the continental slope and rise off North Carolina. *Mar. Pet. Geol.,* 2:260–272.

Day, R., Fuller, M., and Schmidt, V.A., 1977. Hysteresis properties of titanomagnetites: grain-size and compositional dependence. *Phys. Earth Planet. Inter.,* 13:260–267.

Dillon, W.P., and Paull, C.K., 1983. Marine gas hydrates, II. Geophysical evidence. *In* Cox, J.L. (Ed.), *Natural Gas Hydrates: Properties, Occurrences, and Recovery:* Woburn, MA (Butterworth), 73–90.

Gradstein, F.M., and Sheridan, R.E., 1983. Introduction. *In* Sheridan R.E., Gradstein, F.M., et al., *Init. Repts. DSDP,* 76: Washington (U.S. Govt. Printing Office), 5–18.

Heywood, B.R., Bazylinski, D.A., Garratt-Reed, A., Mann, S., and Frankel, R.B., 1990. Controlled biosynthesis of greigite (Fe_3S_4) in magnetotactic bacteria. *Naturwissenschaften,* 77:536–538.

Housen, B.A., and Musgrave, R.J., 1996. Rock-magnetic signature of gas hydrates in accretionary prism sediments. *Earth Planet. Sci. Lett.*, 139:509–519.

Kalcheva, V., Nozharov, P. Kovacheva, M., and Shopov, V., 1990. Paleomagnetic research on Black Sea Quaternary sediments. *Phys. Earth Planet. Inter*., 63:113–120.

Karlin, R., 1990. Magnetite mineral diagenesis in suboxic sediments at Bettis Site W-N, NE Pacific Ocean. *J. Geophys. Res.,* 95:4421–4436.

Leslie, B.W., Lund S.P., and Hammond, D.E., 1990. Rock magnetic evidence for the dissolution and authigenic growth of magnetic minerals within anoxic marine sediments of the California continental borderland. *J. Geophys. Res.,* 95:4437–4452.

Lovley, D., and Phillips, E.J.P., 1988. Novel mode of microbial energy metabolism: organic carbon oxidation coupled to dissimilatory reduction of iron or manganese. *Appl. Environ. Microbiol.,* 54:1472–1480.

Lovley, D.R., Stolz, J.F., Nord, G.L., Jr., and Phillips, E.J.P., 1987. Anaerobic production of magnetite by a dissimilatory iron-reducing microorganism. *Nature,* 330:252–254.

Musgrave, R.J., Collombat, H., and Didenko, A.N., 1995. Magnetic sulfide diagenesis, thermal overprinting, and paleomagnetism of accretionary wedge and convergent margin sediments from the Chile triple junction region. *In* Lewis, S.D., Behrmann, J.H., Musgrave, R.J., and Cande, S.C. (Eds.), *Proc. ODP, Sci. Results,* 141: College Station, TX (Ocean Drilling Program), 59–76.

Musgrave, R.J., Goodman, K., Parkes, R.J., Wellsbury, P., and Kelly, J.C., 1997. Rock-magnetic analysis of deep bacterial iron diagenesis associated with marine gas hydrates. *Eos*, 78:F344.

Paull, C.K., Spiess, F.N., Ussler, W., III, and Borowski, W.A., 1995. Methane-rich plumes on the Carolina continental rise: associations with gas hydrates. *Geology,* 23:89–92.

Popenoe, P., Schmuck, E.A., and Dillon, W.P., 1993. The Cape Fear landslide: slope failure associated with salt diapirism and gas hydrate decomposition. *In* Schwab, W.C., Lee, H.J. and Twichell, D.C., (Eds.), *Submarine Landslides: Selective Studies in the U.S. Exclusive Economic Zone.* U.S. Geol. Surv. Bull., 2002:40–53.

Reynolds, R.L., Tuttle, M.L., Rice, C.A., Fishman, N.S., Karachewski, J.A., and Sherman, D.M., 1994. Magnetization and geochemistry of greigite-bearing Cretaceous strata, North Slope Basin, Alaska. *Am. J. Sci.,* 294:485–528.

Schmuck, E.A., and Paull, C.K., 1993. Evidence for gas accumulation associated with diapirism and gas hydrates at the head of the Cape Fear slide. *Geo-Mar. Lett.,* 13:145–152.

Shipboard Scientific Party, 1994. Site 892. *In* Westbrook, G.K., Carson, B., Musgrave, R.J., et al., *Proc. ODP, Init. Repts.,* 146 (Pt. 1): College Station, TX (Ocean Drilling Program), 301–378.

————, 1996a. Explanatory notes. *In* Paull, C.K., Matsumoto, R., Wallace, P.J., et al., *Proc. ODP, Init. Repts.,* 164: College Station, TX (Ocean Drilling Program), 13–41.

————, 1996b. Introduction. *In* Paull, C.K., Matsumoto, R., Wallace, P.J., et al., *Proc. ODP, Init. Repts.,* 164: College Station, TX (Ocean Drilling Program), 5–12.

————, 1996c. Sites 991/992/993. *In* Paull, C.K., Matsumoto, R., Wallace, P.J., et al., *Proc. ODP, Init. Repts.,* 164: College Station, TX (Ocean Drilling Program), 65–97.

————, 1996d. Site 995. *In* Paull, C.K., Matsumoto, R., Wallace, P.J., et al., *Proc. ODP, Init. Repts.,* 164: College Station, TX (Ocean Drilling Program), 175–240.

————, 1996e. Site 996. *In* Paull, C.K., Matsumoto, R., Wallace, P.J., et al., *Proc. ODP, Init. Repts.,* 164: College Station, TX (Ocean Drilling Program), 241–275.

Shipley, T.H., Houston, M.H., Buffler, R.T., Shaub, F.J., McMillen, K.J., Ladd, J.W., and Worzel, J.L., 1979. Seismic evidence for widespread possible gas hydrate horizons on continental slopes and rises. *AAPG Bull.,* 63:2204–2213.

Snowball, I., and Thompson, R., 1990. A stable chemical remanence in Holocene sediments. *J. Geophys. Res.,* 95:4471–4479.

Tucholke, B.E., Bryan, G.M., and Ewing, J.I., 1977. Gas-hydrate horizons detected in seismic-profiler data from the western North Atlantic. *AAPG Bull.,* 61:698–707.

Date of initial receipt: 24 April 1998
Date of acceptance: 1 March 1999
Ms 164SR-234